Effect of solids on O$_2$ mass transfer in an oscillatory flow reactor provided with smooth periodic constrictions

CrossMark

A. Ferreira [a,*], Patrick O. Adesite [b], J.A. Teixeira [c], F. Rocha [a]

[a] LEPABE-Laboratory for Process Engineering, Environment, Biotechnology and Energy, Departamento de Engenharia Química, Faculdade de Engenharia, Universidade do Porto, Rua Dr. Roberto Frias s/n, 4200-465 Porto, Portugal
[b] Department of Chemical Engineering, Loughborough University, Loughborough, Leicestershire LE11 3TU, United Kingdom
[c] CEB – Centre of Biological Engineering, University of Minho, 4710-057 Braga, Portugal

HIGHLIGHTS

- Mass transfer increase in comparison with conventional gas-liquid contactors.
- Negligible effect of solids on the mass transfer process.
- The presence of solids in the system seems to result in two phenomena.
- Interfacial area increase in three-phase system.
- k^L is influenced by the presence of solids.

ARTICLE INFO

ABSTRACT

In the present work, it is studied for the first time the use of an oscillatory flow reactor provided with smooth period constrictions (OFR-SPC) in gas-liquid mass transfer process when a solid phase is present. The superficial gas velocities (u_G), solids loading (calcium alginate beads: 0–15% (v/v)) and the oscillatory conditions (frequency and amplitude) effects on volumetric liquid side mass transfer coefficient (k_La) are experimentally evaluated. The liquid-side mass transfer coefficient, k_L, and the specific interfacial area, a, are studied individually. The results show that k_La increases with both superficial gas velocity and oscillatory conditions, in two and three-phase systems, the oscillatory conditions being the ones with the highest impact on the gas-liquid mass transfer process. The presence of solids seems to have a negligible influence on k_La in all experimental conditions for the range of solids loading studied. This behavior was not observed in other reactors where a negative solids (calcium alginate beads) influence on the mass transfer process was verified. Globally, the results show the importance of hydrodynamic phenomena on the mass transfer process in two and three-phase systems, indicating OFR-SPC as a good alternative to the conventional reactors, especially when a third phase is present.

© 2016 Elsevier Ltd. All rights reserved.

1. Introduction

In order to create the optimal environment for fermentation, bioreactors must provide the cells access to all substrates. This is a challenging process, as the most of the biotechnology systems are composed by three-phases: gas (e.g. air), liquid (e.g. medium) and solids (e.g. biomaterial, that can be present as immobilized or encapsulated forms) and, ideally, all of these must be perfectly distributed along the different sections of the bioreactor. Airlift, bubble column and stirred tank reactors are the most commonly used devices for enhancing gas-liquid mass transfer and, by this way, are the normal choice in processes involving biomaterial (Doran, 1995; Deckwer, 1992). The type of mixing, heat and mass transfer process characterizes the different reactors, and choosing the best one for a certain application is not an easy task. Despite their popularity in chemical and biological processes, problems related with product quality, process reproducibility and scale up, are typically reported (Vasconcelos et al., 1995; Freitas and Teixeira, 1998; Klein et al., 2003; Mirón et al., 2004; Kumaresan et al., 2005; Fernandes et al., 2014), especially when a third phase is present in the system (Sada et al., 1985, 1986; Freitas and Teixeira, 1998; Mena et al., 2005, 2011). The presence of solids affects the gas-liquid mixture in different ways: bubble formation

---

* Corresponding author.
E-mail address: antonio@fe.up.pt (A. Ferreira).

Nomenclature

A_{proj}	projected bubble area, m^2		N_b	number of baffles per unit length, m^{-1}
A_{sup_i}	bubble superficial area, m^2		n_p	number of points, dimensionless
a	specific interfacial area, m^{-1}		R	empirical constant of Eq. (9), dimensionless
C	oxygen concentration in the liquid, kg/L		R_c	radius of curvature of the sidewall of the convergent subsection, m
C_0	oxygen concentration in the liquid at $t = 0$, kg/L			
C_n	concentration of particles on the nth cell		R_d	radius of curvature of the sidewall of the divergent subsection, m
C^*	oxygen solubility in the liquid, kg/L			
D	inner diameter of the straight section, m		Re_o	oscillatory Reynolds number, dimensionless
D_{eq}	equivalent diameter, m		R_t	radius of curvature of constriction center, m
d_p	particle diameter, m		St	Strouhal number, dimensionless
d_0	internal tube diameter in the constrictions, m		T	temperature, °C
d_{32}	Sauter mean diameter, m		t	time, s
f	oscillation frequency, Hz		u_G	superficial gas velocity, m/s
g	gravitational constant, $m\,s^{-2}$		V_m	maximum oscillation velocity, m/s
H	column height, m		V_s	settling velocity of the particles, m/s
h	liquid height, m		x_0	oscillation amplitude, m
h_0	initial liquid height, m		γ	concentration ration between adjacent cells ($\gamma = C_{n+1}/C_n$), dimensionless
k_L	liquid-side mass transfer coefficient, m/s			
$k_L a$	volumetric liquid side mass transfer coefficient, s^{-1}		v	kinematic viscosity, m^2/s
L	mean spacing between consecutive constrictions, m		ω	angular frequency of oscillation defined as $2\pi f$, Hz
L_1	constriction length, m		ρ	fluid density, $kg\,m^{-3}$
L_2	straight tube length, m		ε_G	gas holdup, dimensionless
n	number of bubbles, dimensionless			

(Yoo et al., 1997; Luo et al., 1998; Fan et al., 1999), bubble rise (Luo et al., 1997; Fan et al., 1999), axial and radial profiles (Warsito et al., 1997; Gandhi et al., 1999; Mena et al., 2008), mixing and dispersion, mass transfer (Quicker et al., 1984; Sada et al., 1985; Joly-Vuillemin et al., 1996; Mena et al., 2005, 2011), and gas holdup and flow regimes (Zhang et al., 1997; Mena et al., 2005; Mena et al., 2008).

In order to overcome some of the limitations identified on the common devices, the oscillatory flow reactors (OFR) have been studied, mainly in two phase systems (Hewgill et al., 1993; Oliveira and Ni, 2004a,b). So far, the influence of the solids in the gas-liquid mass transfer process in OFR is an unexplored area. OFR is basically a column provided with periodic constrictions (baffles, with variable geometric configuration), operating under oscillatory flow mixing (OFM). The liquid or multiphase fluid is typically oscillated in the axial direction by means of diaphragms, bellows or pistons, at one or both ends of the tube, developing an efficient mixing mechanism where fluid moves from the walls to the center of the tube with intensity controlled by the oscillation frequency (f) and amplitude (x_0) (Mackley and Ni, 1991, 1993; Smith, 1999; Fitch and Ni, 2003). The formation and dissipation of eddies, in these reactors, has proved to result into significant enhancement in processes such as heat transfer (Mackley and Stonestreet, 1995), mass transfer (Hewgill et al., 1993; Mackley et al., 1998; Ni et al., 1995; Ni and Gao, 1996; Oliveira and Ni, 2004b), particle mixing and separation (Mackley et al., 1993; McGlone et al., 2015).

The fluid mechanical condition in the OFR is controlled by the oscillatory Reynolds number (Re_o) and the Strouhal number (St), defined as:

$$Re_o = \frac{2\pi f x_0 \rho D}{\mu} \tag{1}$$

$$St = \frac{D}{4\pi x_0} \tag{2}$$

where ρ is the fluid density and μ is the fluid viscosity. The Re_o describes the intensity of mixing applied to the column, and St characterize the effective eddy propagation.

In the last decade a new generation of OFR has been arising, the meso-OFR (McDonough et al., 2015). These mesoscale (milliliter) oscillatory baffled reactors have received considerable attention due to their small volume and ability to operate at low flow rates, reducing reagent requirements and waste. In order to obtain the best mixing several tube diameters (D) (4 mm < D < 6 mm) and baffle designs have been tested at this new scale, in opposition to the conventional OFR (D > 15 mm) where the baffles design is restricted to one type: annular baffles. The smooth periodic constrictions (SCP) baffle design was used, for the first time, by Reis et al. (2007) in gas-liquid mass transfer studies at meso-scale. This baffle design was developed by Reis (2006) for biotechnological applications, in order to reduce the high shear stress regions found near the sharp edges of conventional OFRs, which are critical to some cell cultures. Recently, Ferreira et al. (2015) studied the influence of several geometric parameters that characterize the oscillatory flow reactor provided with smooth period constrictions (OFR-SPC) at meso and macroscale in order to obtain the lowest mixing times. The optimized values obtained were submitted for patent protection and have been applied to gas-liquid (Ferreira et al., 2015) and crystallization systems (Castro et al., 2016).

In the present work, it is studied for the first time the use of an OFR (D = 16 mm) provided with smooth periodic constrictions, in gas-liquid mass transfer process when a solid phase is present. The superficial gas velocities (u_G), solids loading (calcium alginate beads: 0–15% (v/v)) and the oscillatory conditions (frequency and amplitude) effects on volumetric liquid side mass transfer coefficient ($k_L a$) are experimentally evaluated. The liquid-side mass transfer coefficient, k_L, and the specific interfacial area, a, are studied individually.

The methodology adopted in the present work aims to open new insights for a better understanding of mass transfer phenomena in the OFR-SPC when a solid phase is present.

2. Experimental facilities and procedure

2.1. Experimental apparatus

Mass transfer experiments were performed in the oscillatory flow reactor provided with smooth periodic constrictions (OFR-SPC) made of glass (Fig. 1). The reactor inner diameter (D) is 1.6 cm and has 50 cm in height providing a total volume of ~70 mL. The SPC dimensions are in the range presented on Ferreira et al. patent application (Ferreira et al., 2015). Temperature was regulated by a water jacket and a thermostatic bath, maintained at 25 °C.

The fluid was oscillated using an oscillatory device, purposely designed. Oscillation amplitudes (x_0) and frequencies (f) ranged from 0.07 to $0.34 \times L$ and 1 to 4 Hz, respectively. L is the mean spacing between consecutive constrictions ($L = L_1 + L_2$). Values of the amplitudes correspond to the center-to-peak amplitude and these measurements were performed in the tube without constrictions. A single needle gas sparger was used allowing the formation of small, uniform and distinct bubbles. The superficial gas velocities, u_G, range from 0.1 to 10 mm/s. According to the operating conditions used Re_o presents values corresponding to the laminar ($Re_o < 2300$), transition ($2300 < Re_o < 4000$) and turbulent ($Re_o > 4000$) flow regimes, and St values up to 0.5.

Fig. 1. Schematic diagram of the experimental apparatus. D – inner diameter of the straight section; d_0 – internal tube diameter in the constrictions; L_1 – constriction length; L_2 – straight tube length; R_c – radius of curvature of the sidewall of the convergent subsection; R_d – radius of curvature of the sidewall of the divergent subsection; R_t – radius of curvature of constriction center.

2.2. Mass transfer experiments – methodology

Oxygen mass transfer experiments were performed in two and three-phase systems at constant temperature (25 °C) and different superficial gas velocities (up to 10 mm/s) controlled by precision gas mass flow controllers (Alicat scientific). Distilled water and air K were used as liquid and gas phase, respectively. The solids used were calcium alginate beads with an average equivalent diameter (d_p) of 1.2 mm and density $\rho_p = 1023$ kg/m³. To produce the calcium alginate beads, with a roughly spherical shape, a $2\%(w/v)$ sodium alginate solution was prepared dissolving sodium alginate in water at a temperature higher than 70 °C, under strong agitation. This mixture was then dropped into a 2% (w/v) calcium chloride solution using a 0.45 mm outer diameter needle; calcium alginate beads were formed by ion exchange $Ca^{2+} \leftrightarrow Na^+$. An electric impulse generator working at 9 kV was connected to the chamber where the needle is fixed to promote very small drops that result in smaller beads (Mena et al., 2005). The equivalent diameter of the beads was measured as follows: several images of a considerable amount of particles were obtained from a digital camera coupled with a microscope and then the images were automatically analyzed, according to a methodology similar to the one described in Section 2.3, and the bead size obtained based on its projected area (Eq. (5)).

The choice of this solid phase corresponds to the scientific interest in three-phase reactors with immobilized biomass. The solids are well-defined completely wettable objects with reasonable rigidity that do not form agglomerates and are big enough not to affect the surface properties of the gas-liquid interface.

The liquid height was $h_0 = 45$ cm for all experiments (no liquid throughput).

Initially the liquid is deoxygenated by bubbling nitrogen. When the dissolved oxygen concentration is practically zero, air is fed into the column. At this moment the oxygen transfer process from bubbles to the liquid begins and continues until oxygen concentration in the liquid reaches the saturation. Dissolved oxygen concentration values were measured online using an fiberoptic oxygen meter (OXR50-HS, Pyroscience – error in reading was ±0.01–0.1 mg O_2/l), located 0.35 m from the gas sparger and 0.5 D from the wall, connected to the FireSting O_2 instrument (Pyroscience), and recorded directly in a PC, through the FireSting Logger software. No bubbles interference on the probe measurements was observed. By this way, the dissolved oxygen concentration variation with time, t, is obtained, and $k_L a$ can be calculated according to the following procedure.

The mass balance for oxygen in the liquid is written as:

$$\frac{dC}{dt} = k_L a(C^* - C) \tag{3}$$

where C^* and C are, respectively, the oxygen solubility and oxygen concentration in the liquid. Assuming the liquid phase homogeneous and C_0 the oxygen concentration at $t = 0$, the integration of the previous equation leads to:

$$\ln(C^* - C) = \ln(C^* - C_0) - k_L a \cdot t. \tag{4}$$

The volumetric mass transfer coefficient can now be determined by plotting $\ln(C^* - C)$ against time (t).

Typically, the dissolved oxygen concentration during the aeration has two distinguished zones, one with an intense mass transfer zone where the O_2 concentration rises fast and other close to the saturation, when the mass transfer rate starts to decline. As previously mentioned, plotting $\ln(C^* - C)$ against time, $k_L a$ can be determined from the slope in the linear zone. In order to define this zone by a statistic way, the statistical method Test F (Hoel, 1976) was used. This method consists in the determination of the opti-
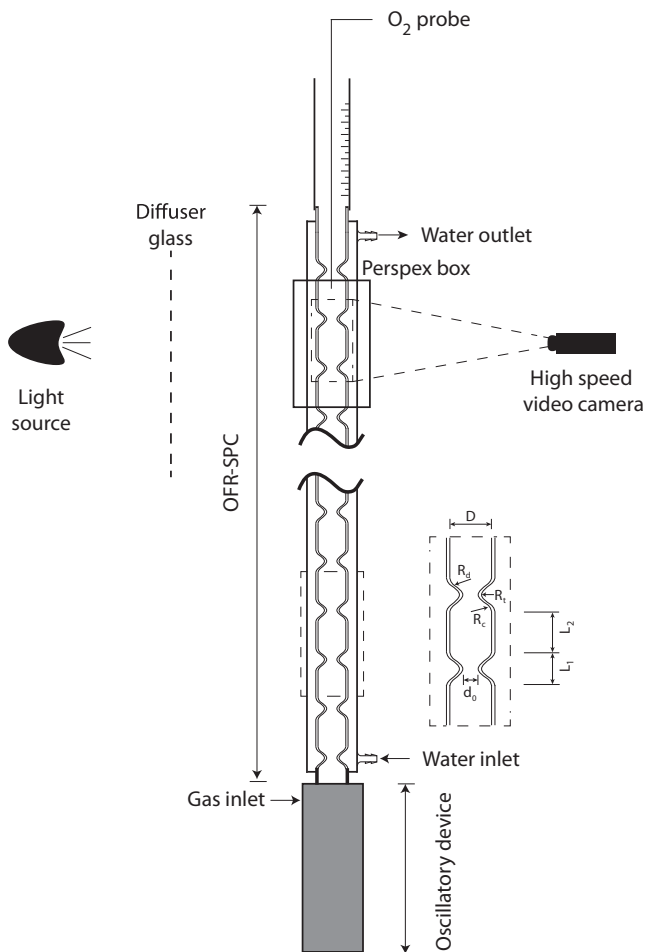
mum number of points (n_p) for a linear regression of experimental data (Mena et al., 2011). The solubility of oxygen in water (C^*) was taken experimentally for each run by using the average of the last ten values of the dissolved oxygen concentration in the saturation zone (it was assumed that the system is saturated when no change on the dissolved oxygen concentration is observed during a period of 15 min.).

The experimental results are reproducible with an average relative error of 5% and are not influenced by the dynamics of the oxygen electrode since its response time, less than 0.8 s for a 90% confidence interval (technical data), was much smaller than the mass transfer time of the system (ranging from 6 to 170 s). The claimed average relative error of 5% was calculated from five runs (at same experimental conditions).

2.3. Bubble size distribution and mean bubble size

As in Ferreira et al. work (Ferreira et al., 2015), in order to obtain the bubble size distribution a Perspex rectangular box was fitted at mid-height of the OFR-SPC and filled with water, as shown in Fig. 1. This box minimizes the optical distortion of the OFR-SPC wall curvature. Sets of images were grabbed with a black and white high speed digital video camera (frame rate of 250 images/s) connected to a PC, in the same conditions of k_La determinations. After the acquisition a set of images (about 5 images/s) are automatically treated and the bubbles are identified and classified according to the methodology developed by Ferreira et al. (2012). With the previous methodology, the automatic identification of single bubbles (isolated bubbles without influence of surrounded bubbles) at dif-
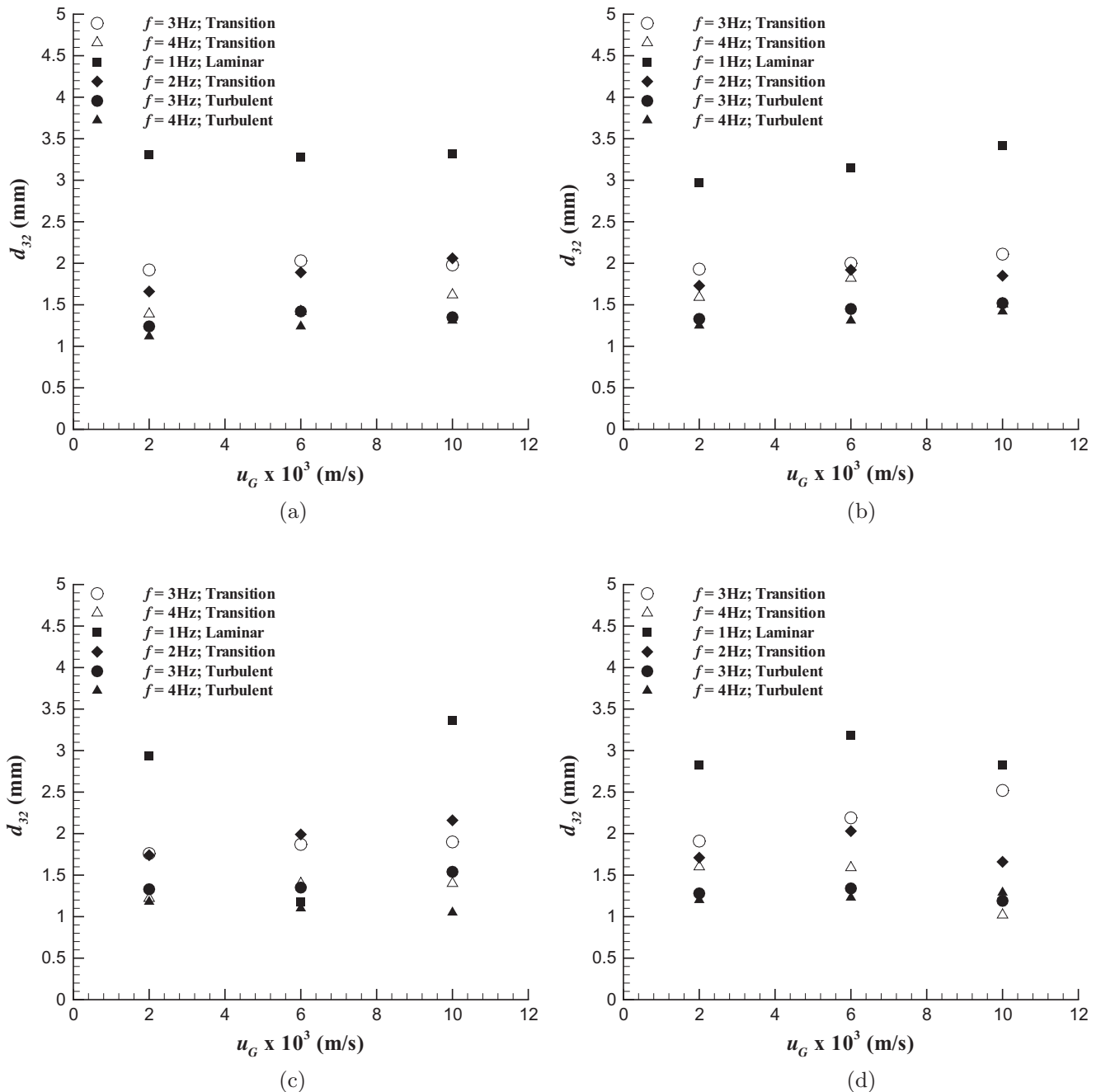

Fig. 2. Effect of oscillation frequency and superficial gas velocity on Sauter mean diameter in the OFR-SPC at different amplitudes (empty shape signifies $x_o = 0.17 \times L$; filled shaped signifies $x_o = 0.34 \times L$) and calcium alginate beads ($d_p = 1.2$ mm) concentrations (v/v): (a) 0%; (b) 5%; (c) 10%; (d) 15%. Identification of the different flow regimes.

ferent operational conditions was possible in two and three-phase systems. The automatic and correct characterization of the single bubbles allows the correct determination of bubble size and, consequently, the specific interfacial area a.

The bubbles produced are, mostly, close to the spherical geometry. So, the size of each individual bubble (D_{eq_i}) was quantified from the projected bubble area according to the following equation:

$$D_{eq_i} = \sqrt{\frac{4 \cdot A_{proj_i}}{\pi}} \tag{5}$$

For processes involving mass transfer through an interfacial area, the bubble size distribution (BSD) is well represented by the Sauter mean diameter (d_{32}) which is given by

$$d_{32} = \frac{\sum_i n_i \cdot D_{eq_i}^3}{\sum_i n_i \cdot D_{eq_i}^2} \tag{6}$$

According to Ferreira et al. (2012) an relative error less than 3% is expected in bubble size measurement, using the previous methodology, for columns with reduced diameters (around 20 mm). Since in present work the column diameter is 16 mm, it was assumed the same relative error.

2.4. Gas holdup and specific interfacial area

The volume fraction of the gas phase (gas holdup, ε_G) was measured by recording the changes in the liquid height in the OFR-SPC using a digital video camera together with a fine scale fixed on the
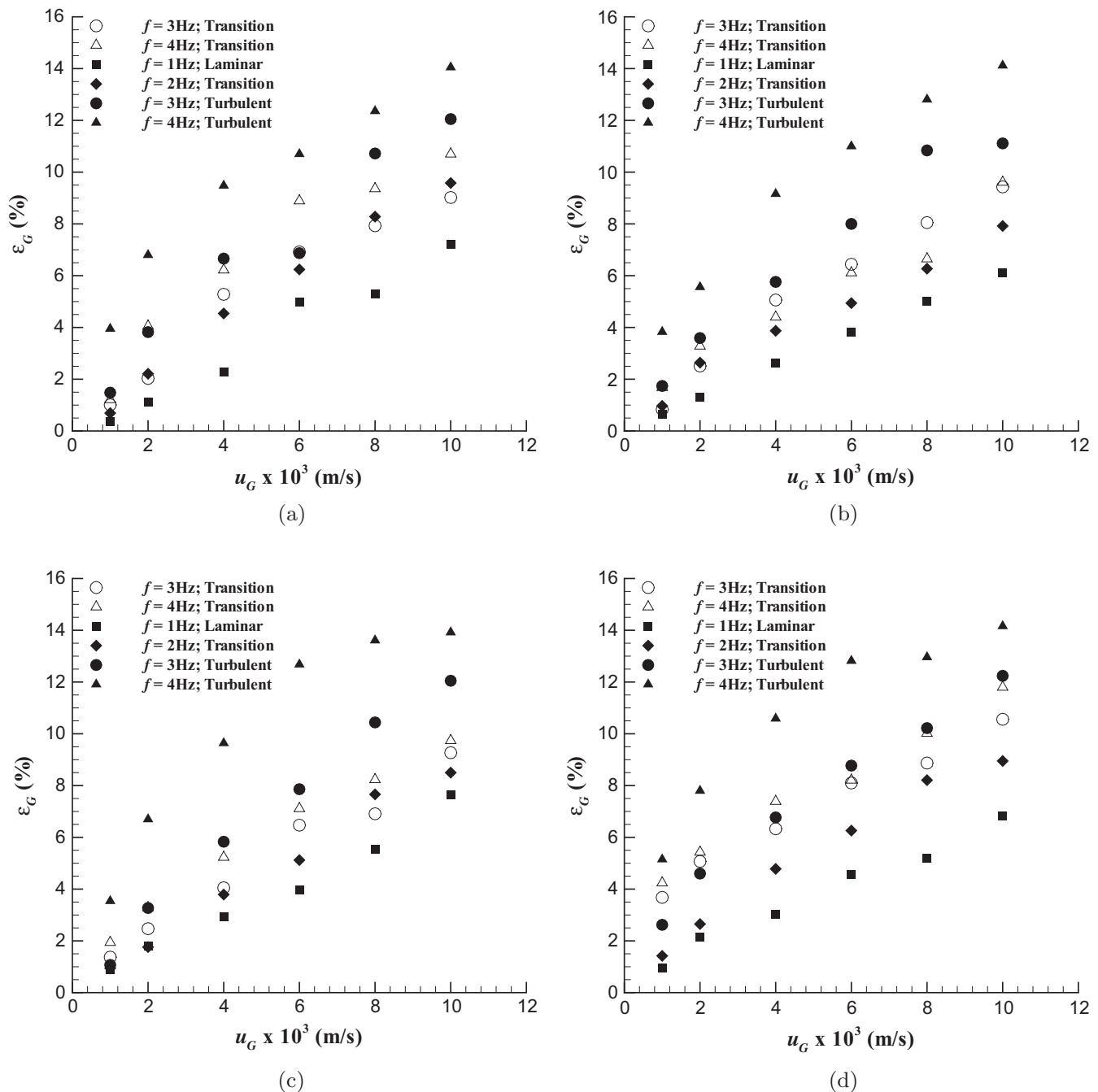

Fig. 3. Effect of oscillation frequency and superficial gas velocity on gas holdup in the OFR-SPC at different amplitudes (empty shape signifies $x_o = 0.17 \times L$; filled shaped signifies $x_o = 0.34 \times L$) and calcium alginate beads ($d_p = 1.2$ mm) concentrations (v/v): (a) 0%; (b) 5%; (c) 10%; (d) 15%. Identification of the different flow regimes.

top of the column. The procedure involves measuring the liquid level without the presence of gas, h_0, and the corresponding level, h, when gas is continuously introduced in the column at a given flow rate and oscillatory conditions (x_0 and f). In order to reduce the error associated to the h measurement an average of 10 values was used for all experimental conditions. The gas holdup is calculated from the volume variation by the following equation:

$$\varepsilon_G = \frac{h - h_0}{h} \tag{7}$$

The relative error associated to the ε_G measurements is less than 14% for $u_G \geqslant 0.2$ cm/s. The claimed error is the upper limit for voidage error in the range measured. The liquid layer can be located with precision of 0.5 mm (resolution of the scale). For layers with liquid height (h) $\approx$45.5–52.4 cm (voidage 1.1–14.2%), an error of 0.11–0.09% in h is obtained, which causes an relative error of 14–1%, respectively, in ε_G.

Based on gas holdup, ε_G, and the BSD measurements the specific interfacial area, a, was determined as follows:

$$a = 6 \frac{\varepsilon_G}{d_{32}} \tag{8}$$

and a range of relative errors (3–14.2%) in a was obtained.

2.5. Particle suspension

The effect of oscillatory flow in baffled tubes on particle suspension was studied by Mackley et al. (1993). According to the authors an uniform suspension of particles can be obtained by controlling the frequency and amplitude of oscillation. The particles suspension on Mackley et al. (1993) work were characterized by the following empirical correlation:

$$\gamma = \left[1 - \exp\left(-R \frac{V_m}{V_s} \right) \right] \tag{9}$$

where γ is the concentration ratio between adjacent cells ($\gamma = C_{n+1}/C_n$, where C_n is the concentration of particles on the nth cell), V_m is the maximum oscillation velocity ($= x_0\omega = x_0 2\pi f$) (ms^{-1}), V_s is the settling velocity of the particles (ms^{-1}) and R an empirical constant. When $\gamma \approx 1$ a uniform particle suspension is achieved in the OFR. However, when $\gamma < 1$ (achieved by varying V_m) a particle concentration gradient can be obtained (Ni et al., 2003).

3. Results and discussion

A common behavior observed at low u_G and oscillatory conditions (low f and x_0) was the phenomenon of particle sedimentation, leading to a concentration gradient along the length of the OFR-SPC. Such behavior could result in an unrepresentative bubble coalescence and, consequently, to an unrepresentative mass transfer phenomenon in a given solid concentration. According to the literature (Mackley et al., 1993), a uniform particle suspension is achieved in the OFR when $\gamma \approx 1$. Upon observation at different amplitudes, $x_0 = 0.07 \times L$, at all frequencies, and $x_0 = 0.17 \times L$, at 1 and 2 Hz, show a deficient solid suspension. For these oscillatory conditions the value of γ in Eq. (9) is $\gamma \ll 1$ which is ideal for separating particles of different sizes and densities. By this way, theses conditions were not used on studies concerning the effect of solids (calcium alginate beads ($d_p = 1.2$ mm)) on mass transfer in the OFR.

3.1. Bubble size distribution and mean bubble size

When the oscillatory motion is applied in the OFR several bubble behaviors are promoted, being the bubble coalescence and

breakage, bubble velocity reduction and bubble trap within each baffled-cell being the most significant. The prevalence of one over another depends on the operating conditions. Fig. 2 shows the effect of the operating conditions and solid loading on the Sauter mean diameter. As it is observed, the highest bubbles sizes are obtained at laminar flow regime ($Re_o < 2300$). When the oscillatory motion is increased a transition ($2300 < Re_o < 4000$) and turbulent flow ($Re_o > 4000$) regimes are obtained, and a consequent bubble size reduction is observed. According to the experimental results, the bubbles size behavior in the OFR without solids is similar to Ferreira et al. (2015) work, being the small differences observed related with the gas sparger used on the present work. The presence of the solid phase (calcium alginate beads ($d_p = 1.2$ mm)) seems to not affect the d_{32} behavior at different operating conditions. This is a remarkable result. Mena et al. (2005), using the same type of particles in a bubble column, report significant solid effect on the d_{32}, observing a d_{32} increasing as the solid loading is increased. Comparing the two reactors (OFR and bubble column) operating at the same experimental conditions (temperature, gas flow rate, solid type, size and loading), it seems that the oscillatory motion reduces the bubble coalescence phenomenon observed in the bubble column when a solid phase is present.

3.2. Gas holdup

The measurements of gas holdup as a function of superficial gas velocity, oscillatory conditions and solid loading are plotted in Fig. 3(a)–(c). As one can see the gas holdup is influenced by the variables superficial gas velocity and oscillatory conditions. Increasing the superficial gas velocity results in a ε_G increase. In what concern the oscillatory conditions, it seems that both frequency and amplitude play a crucial role on ε_G, being the effect of oscillation frequency on ε_G more pronounced at high amplitude. According to Ferreira et al. (2015) work, on the same type of oscillatory flow reactor, this behavior is related with bubble trap within each baffled-cell increasing its radial velocity and, consequently, its average residence time. These observations are in agreement with Oliveira et al. (2003,) conclusions, using the conventional OFR, i.e. without SPC.

It can be also observed that the presence of the solid phase (calcium alginate beads ($d_p = 1.2$ mm)) seems to enhance the ε_G
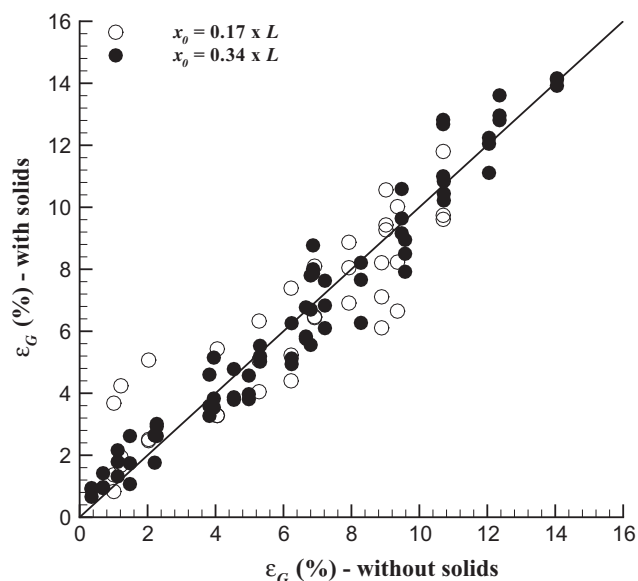

Fig. 4. Effect of calcium alginate beads ($d_p = 1.2$ mm) on gas holdup.

(Fig. 4). For the higher amplitude, an increase of 2%, 7% and 25% (on average) was achieved, when a solid loading of 5%, 10% and 15%, respectively, is used. Using the lower amplitude the enhancement in ε_G was just verified at the higher solid concentration. At these conditions an increase of 66% (on average) was obtained, this value being a result of the enormous influence of the solids on the gas holdup at low flow rates (less than 0.6 cm/s). Despite the experimental errors associated to ε_G it seems that, globally, the solids act positively on ε_G. An opposite effect of the solids on ε_G was observed by Mena et al. (2005), using the same type of particles and size, in a bubble column. These different behaviors seem to be related to the oscillatory motion that, by one way, produces small bubbles (less than 3 mm) that seems not to be significantly affected by the presence of solids and, by other way, the solids

reduce the bubbles rise velocity that become trapped within each baffled-cell resulting in an gas holdup increase.

3.3. Mass transfer

Fig. 5 shows the effect of oscillation frequency and superficial gas velocity on volumetric liquid side mass transfer coefficient in the OFR-SPC at different amplitudes and solid loading. It can be seen from this figure that k_La increases with superficial gas velocity and it is strongly dependent on the intensity of mixing applied to the system. An increase in the oscillation conditions leads to an increases in k_La, being the amplitude the variable with the highest impact on k_La, since the oscillation amplitude controls the length of the eddy generated along the column that has a strong impact
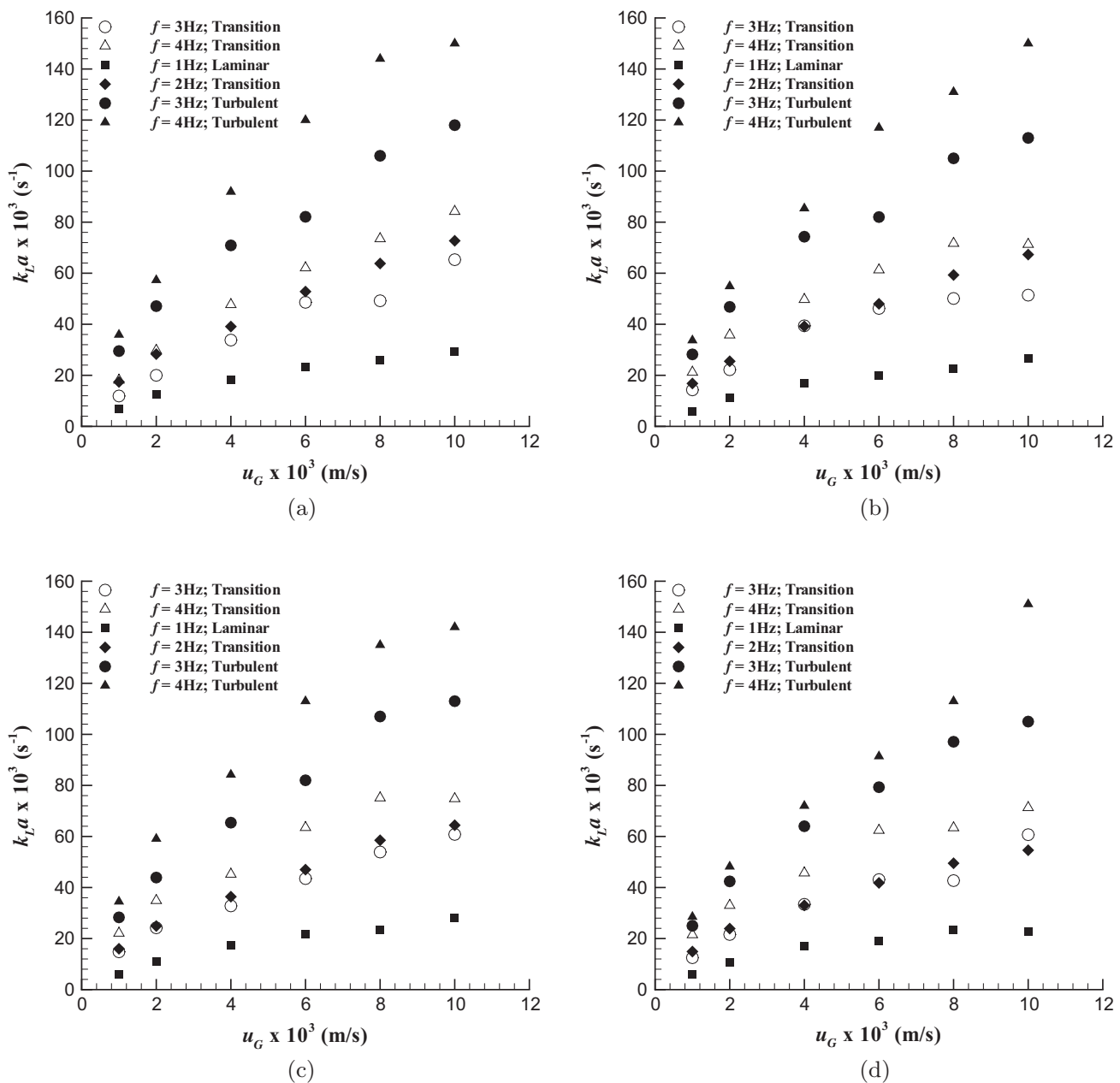

Fig. 5. Effect of oscillation frequency and superficial gas velocity on volumetric liquid side mass transfer coefficient in the OFR-SPC at different amplitudes (empty shape signifies $x_o = 0.17 \times L$; filled shaped signifies $x_o = 0.34 \times L$) and calcium alginate beads ($d_p = 1.2$ mm) concentrations (v/v): (a) 0%; (b) 5%; (c) 10%; (d) 15%. Identification of the different flow regimes.
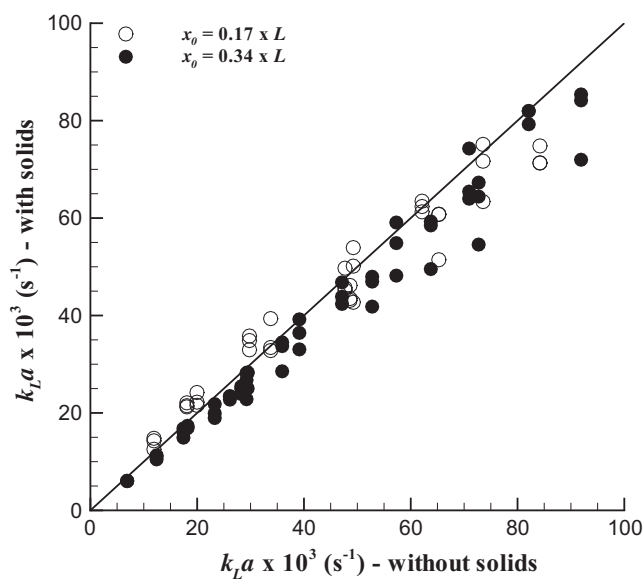
Fig. 6. Effect of calcium alginate beads ($d_p = 1.2$ mm) on volumetric liquid side mass transfer coefficient.

on bubble behavior within the OFR-SPC. According to Fig. 6, where is plotted a comparison between the k_La values obtained in presence and absence of solids (calcium alginate beads ($dp = 1.2$ mm)) at the same operating conditions, the presence of solids seems to have a negligible influence on k_La in all experimental conditions for all range of solid loading studied. The highest deviation observed was 9%. Considering the experimental error associated to the k_La values (around 5%) the previous conclusion, concerning the negligible influence of the solids on k_La, seems to be valid.

This negligible solid influence on k_La was not observed in other reactors, where a negative solids influence on the mass transfer process was obtained, using the same type of solids (calcium alginate beads ($d_p = 1.2$ mm)). Mena et al. (2005) observe a significant solid effect on the k_La using just 10% of solids in a bubble column; the same behavior was observed by Freitas and Teixeira (2001) using calcium alginate beads with an equivalent diameter of 2.1 mm in an internal loop airlift reactor.

3.4. Specific interfacial area and liquid-side mass transfer coefficient

In order to evaluate the effect of the studied parameters on a and k_L separately, the specific interfacial area was determined using the ε_G and d_{32}, as already described, and the results were combined with the k_La values at the same experimental conditions. In order to show the solid phase (calcium alginate beads ($d_p = 1.2$ mm)) influence on a and k_L by a simple way, it was chosen on this work to present just a specific range of experiments.

Fig. 7(a) shows the effect of oscillation frequency and superficial gas velocity on a at different amplitudes and constant solid concentration (15%). As one can see the specific interfacial area is influenced by the superficial gas velocity and oscillatory conditions. Increasing the superficial gas velocity results in a specific interfacial area increase. The same occurs when the amplitude and frequency are increased. It seems that both frequency and amplitude play a crucial role on a, being the effect of oscillation frequency on a more pronounced at high amplitude. At that extreme conditions (high frequency and amplitude), the solid loading influence on a was studied (Fig. 7(c)). As one can see, globally, an increase in the solid loading results in an increase in the specific

interfacial area. The presence of solids in the system reduces the bubble rise velocity that become trapped within each baffled-cell resulting in an specific interfacial area increase. Regarding the solids influence on k_L (Fig. 7(d)), one can see that a solid loading increase leads to a k_L decrease, being these results in agreement with Mena et al. (2005) work. This behavior can be related to a decrease in the renewal rate of the liquid film at the bubbles interface when a solid phase is present, conducting, by this way, to a k_L decrease. According to Fig. 7(b), where it is shown the effect of oscillation frequency and superficial gas velocity on k_L at different amplitudes and constant solid concentration (15%), increasing the frequency results in a k_L decrease, being this effect enhanced at high amplitudes and low u_G. This effect is opposite to the one observed in two-phase systems (Ferreira et al., 2015), where a k_L increase with a oscillatory motion was verified. Combining the literature data with the present results it can be inferred that the bubbles trapped in vortices suffer an increase in the renewal rate of the liquid film at the interface conducting to a k_L increase just when a solid phase is not present. In those conditions, the presence of solids starts to decrease the micro mixing at the bubble interface reducing the renewal rate of the liquid film, resulting in a k_L decrease.

In what concerns to the superficial gas velocity influence on k_L when the solid phase (calcium alginate beads ($d_p = 1.2$ mm)) is present, it can be concluded that, globally, k_L decreases with the superficial gas velocity, being this effect reduced at high oscillatory motion ($x_o = 0.34 \times L$, $f = 4$ Hz). This phenomenon is related with the influence of the other bubbles on the oxygen concentration profiles surrounding the individual bubbles. The amount of small bubbles resulting from the oscillatory motion increase is much greater at high superficial velocities, resulting in a significant influence of one bubble on the mass transfer process of the others, a phenomenon that has been studied by different authors (Koynov et al., 2005; Ferreira et al., 2012). According to the literature, in bubble swarms, bubbles no longer travel by themselves, but rather in liquid perturbed by the wakes of neighboring bubbles. The concentration of gas dissolved in the liquid around the bubble in a swarm no longer depends only on the mass transfer from the bubble itself, but also on the mass transfer from the other bubbles in the swarm. These two factors result in a decrease of the mass transfer coefficient of the bubble swarm compared with a single bubble. This phenomenon was observed and quantified by Ferreira et al. (2012) in a bubble column and the same behavior was observed by Ferreira et al. (2015) in an OFR.

4. Conclusions

The gas-liquid mass transfer process in presence of a solid phase (calcium alginate beads ($d_p = 1.2$ mm)) was investigated for the first time in an oscillatory flow reactor (OFR) provided with smooth periodic constrictions (SPC) operating in batch mode. The main purpose of this work was to analyze the effect of solids on k_La in the OFR-SPC, identifying the contribution of its individual parameters, k_L and a, on mass transfer process.

According to the experimental results, k_La increases with superficial gas velocity and it is strongly dependent on the intensity of mixing applied to the system. An increase in the oscillation conditions leads to an increase in k_La, being the amplitude the variable with the highest impact on k_La, since the oscillation amplitude controls the length of the eddy generated along the column having a strong impact on bubble behavior within the OFR-SPC. The increase in the oscillation motion (frequency and amplitude) results in a bubble size reduction, in a bubble average residence time increase and, consequently, in an ε_G and interfacial area increase. The presence of the solid phase (calcium alginate beads
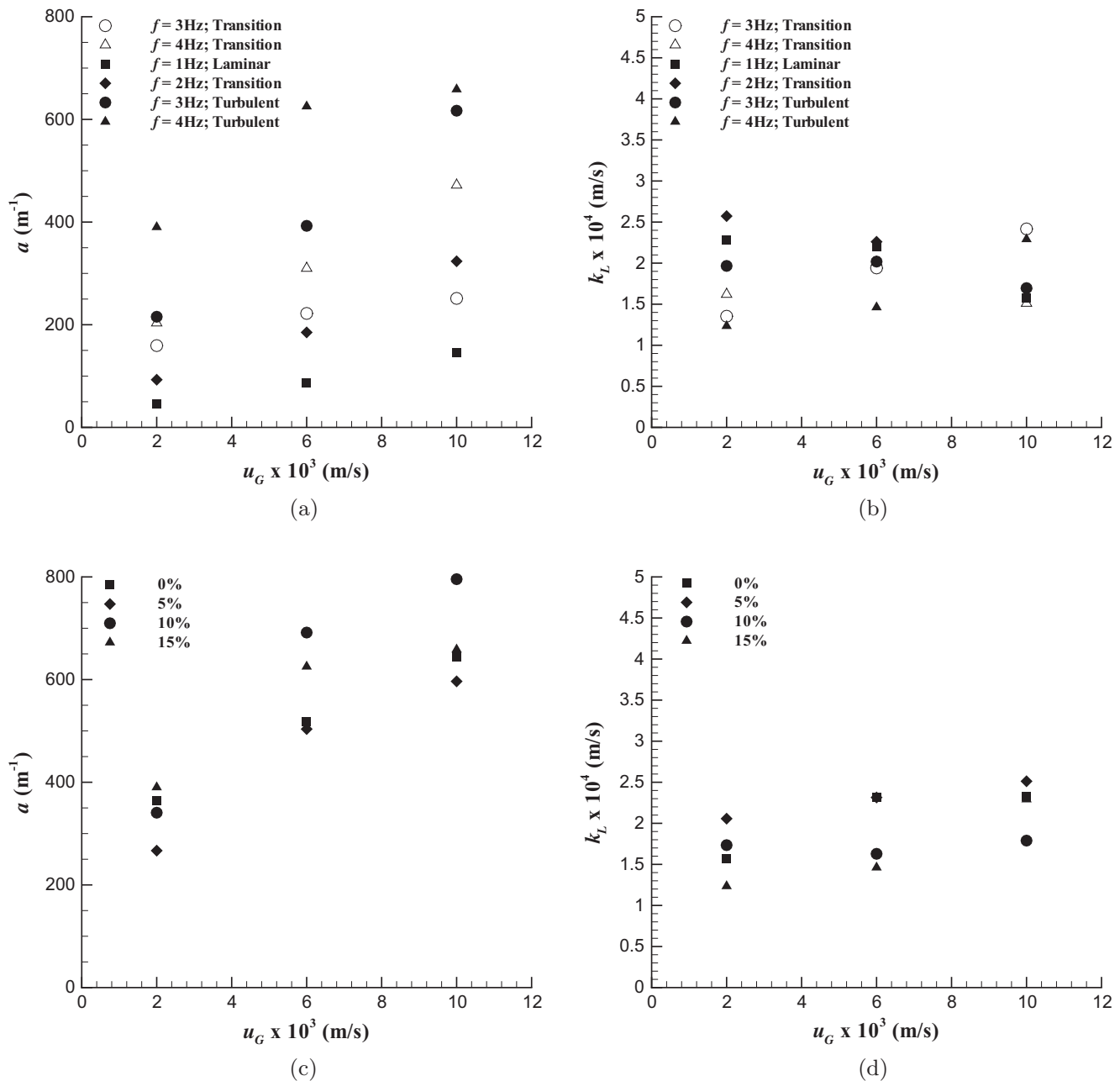
Fig. 7. Effect of oscillation frequency and superficial gas velocity on a (a) and k_L (b) at different amplitudes (empty shape signifies $x_o = 0.17 \times L$; filled shaped signifies $x_o = 0.34 \times L$) and constant calcium alginate beads ($d_p = 1.2$ mm) concentration (15%); and the effect of calcium alginate beads ($d_p = 1.2$ mm) concentrations on a (c) and k_L (d) at constant frequency (4 Hz) and amplitude ($x_o = 0.34 \times L$). Identification of the different flow regimes.

($d_p = 1.2$ mm)) has a negligible influence on $k_L a$ in all experimental conditions for all range of solid loading studied. These results are opposite to the ones observed in the common bioreactors (bubble column and airlift) where a significant solid influence on the mass transfer process was observed. From the individual characterization of a and k_L it can be concluded that the negative effect of the solids was just verified in k_L. The presence of solids in the system seems to results in two phenomena: (1) the solids reduce the bubble rise velocity that become trapped within each baffled-cell resulting in a specific interfacial area increase; (2) the presence of solids decreases the renewal rate of the liquid film at the bubbles interface, conducting to a k_L decrease. The conjugation of these two phenomena results in a negligible influence of the solids on $k_L a$, a remarkable characteristic with potential impact on the bioindustry.

In summary, the present work opens new insights for a better understanding of mass transfer phenomena in the OFR when a solid phase is present and shows that the OFR-SPC is a good alternative to the conventional bioreactors.

Acknowledgements

References

Castro, F., Ferreira, A., Teixeira, J., Rocha, F., 2016. Protein crystallization as a process step in a novel meso oscillatory flow reactor: study of lysozyme phase behavior. Crystal Growth Des. 16, 3748–3755.

Deckwer, W.D., 1992. Bubble Column Reactors. J. Wiley.

Doran, P.M., 1995. Bioprocess Engineering Principles. Elsevier Science.

Fan, L.-S., Yang, G.Q., Lee, D.J., Tsuchiya, K., Luo, X., 1999. Some aspects of high-pressure phenomena of bubbles in liquids and liquid-solid suspensions. Chem. Eng. Sci. 54, 4681–4709.

Fernandes, B.D., Mota, A., Ferreira, A., Dragone, G., Teixeira, J.A., Vicente, A.A., 2014. Characterization of split cylinder airlift photobioreactors for efficient microalgae cultivation. Chem. Eng. Sci. 117, 445–454.

Ferreira, A., Pereira, G., Teixeira, J., Rocha, F., 2012. Statistical tool combined with image analysis to characterize hydrodynamics and mass transfer in a bubble column. Chem. Eng. J. 180, 216–228.

Ferreira, A., Rocha, F., Teixeira, J.A., Vicente, A., 2015. Apparatus for mixing improvement based on oscillatory flow reactors provided with smooth periodic constrictions, WO/2015/056156.

Ferreira, A., Teixeira, J., Rocha, F., 2015. O$_2$ mass transfer in an oscillatory flow reactor provided with smooth periodic constrictions. Individual characterization of kL and a. Chem. Eng. J. 262, 499–508.

Fitch, A.W., Ni, X., 2003. On the determination of axial dispersion coefficient in a batch oscillatory baffled column using laser induced fluorescence. Chem. Eng. J. 92, 243–253.

Freitas, C., Teixeira, J.a., 1998. Effect of liquid-phase surface tension on hydrodynamics of a three-phase airlift reactor with an enlarged degassing zone. Bioprocess. Eng. 19 (6), 451–457.

Freitas, C., Teixeira, J.A., 1998. Hydrodynamic studies in an airlift reactor with an enlarged degassing zone. Bioprocess. Eng. 18 (4), 267.

Freitas, C., Teixeira, J.A., 2001. Oxygen mass transfer in a high solids loading three-phase internal-loop airlift reactor. Chem. Eng. J. 84 (1), 57–61.

Gandhi, B., Prakash, A., Bergougnou, M.A., 1999. Hydrodynamic behaviour of slurry bubble column at high solids concentrations. Powder Technol. 103, 80–94.

Hewgill, R., Mackley, M.R., Pandit, A.B., Pannu, S.S., 1993. Enhancement of gas-liquid mass transfer using oscillatory flow in a baffled tube. Chem. Eng. Sci. 48 (4), 799–809.

Hoel, P.G., 1976. Elementary Statistics. John Wiley & Sons Inc., Australia.

Joly-Vuillemin, C., de Bellefon, C., Delmas, H., 1996. Solid effects on gas-liquid mass transfer in three-phase slurry catalytic hydrogenation of adiponitrile over raney nickel. Chem. Eng. Sci. 51, 2149–2158.

Klein, J., Vicente, A., Teixeira, J., 2003. Hydrodynamic considerations on optimal design of a three-phase airlift bioreactor with high solids loading. J. Chem. Technol. Biotechnol. 78, 935–944.

Koynov, A., Khinast, J.G., Tryggvason, G., 2005. Mass transfer and chemical reactions in bubble swarms with dynamic interfaces. AIChE J. 51 (10), 2786–2800.

Kumaresan, T., Nere, N.K., Joshi, J.B., 2005. Effect of impeller design on the flow pattern and mixing in stirred tanks. Ind. Eng. Chem. Res. 44 (26), 9951–9961.

Luo, X., Zhang, J., Tsuchiya, K., Fan, L.S., 1997. On the rise velocity of bubbles in liquid-solid suspensions at elevated pressure and temperature. Chem. Eng. Sci. 52, 3693–3699.

Luo, X., Yang, G., Lee, D.J., Fan, L.S., 1998. Single bubble formation in high pressure liquid-solid suspensions. Powder Technol. 100, 103–112.

Mackley, M., Ni, X., 1991. Mixing and dispersion in a baffled tube for steady laminar and pulsatile flow. Chem. Eng. Sci. 46 (12), 3139–3151.

Mackley, M., Ni, X., 1993. Experimental fluid dispersion measurements in periodic baffled tube arrays. Chem. Eng. Sci. 48 (18), 3293–3305.

Mackley, M., Stonestreet, P., 1995. Heat-transfer and associated energy dissipation for oscillatory flow in baffled tubes. Chem. Eng. Sci. 50 (14), 2211–2224.

Mackley, M., Smith, K., Wise, N., 1993. The mixing and separation of particle suspensions using oscillatory flow in baffled tubes. Chem. Eng. Res. Des. 71 (A6), 649–656.

Mackley, M.R., Stonestreet, P., Thurston, N.C., Wiseman, J.S., 1998. Evaluation of a novel self-aerating, oscillating baffle column. Can. J. Chem. Eng. 76 (1), 5–10.

McDonough, J., Phan, A.N., Harvey, A.P., 2015. Rapid process development using oscillatory baffled mesoreactors – a state-of-the-art review. Chem. Eng. J. 265, 110–121.

McGlone, T., Briggs, N.E.B., Clark, C.A., Brown, C.J., Sefcik, J., Florence, A.J., 2015. Oscillatory Flow Reactors (OFRs) for continuous manufacturing and crystallization. Organic Process Res. Dev. 19 (9), 1186–1202.

Mena, P.C., Rocha, F.A., Teixeira, J.A., Drahos, J., Ruzicka, M.C., Drahoš, J., 2005. Effect of solids on homogeneous-heterogeneous flow regime transition in three-phase bubble columns. Chem. Eng. Sci. 60 (22), 6013–6026.

Mena, P.C., Pons, M.C., Teixeira, J.A., Rocha, F.A., 2005. Using image analysis in the study of multiphase gas absorption. Chem. Eng. Sci. 60 (18), 5144–5150.

Mena, P.C., Rocha, F.A., Teixeira, J.A., Cartellier, A., Sechet, P., 2008. Measurement of gas phase characteristics using a monofiber optical probe in a three-phase flow. Chem. Eng. Sci. 63 (16), 4100–4115.

Mena, P., Ferreira, A., Teixeira, J.A., Rocha, F., 2011. Effect of some solid properties on gas-liquid mass transfer in a bubble column. Chem. Eng. Process. 50 (2), 181–188.

Mirón, A.S., García, M.-C.C., Camacho, F.G., Grima, E.M., Chisti, Y., 2004. Mixing in bubble column and airlift reactors. Chem. Eng. Res. Des. 82 (A10), 1367–1374.

Ni, X., Gao, S., 1996. Scale-up correlation for mass transfer coefficients in pulsed baffled reactors. Chem. Eng. J. 63, 157–166.

Ni, X., S, G., Cumming, R., DW, P., 1995. A comparative-study of mass-transfer in yeast for a batch pulsed baffled bioreactor and a stirred-tank fermenter. Chem. Eng. Sci. 50 (13), 2127–2136.

Ni, X., Mackley, M.R., Harvey, A.P., Stonestreet, P., Baird, M.H.I., Rao, N.V.R., 2003. Mixing through oscillations and pulsations – a guide to achieving process enhancements in the chemical and process industries. Chem. Eng. Res. Des. 81 (A3), 373–383.

Oliveira, M.S.N., Ni, X.-W., 2004a. Characterization of a gas-liquid OBC: bubble size and gas holdup. AIChE J. 50 (12), 3019–3033.

Oliveira, M.S.N., Ni, X.-w., 2004b. Effect of hydrodynamics on mass transfer in a gas-liquid oscillatory baffled column. Chem. Eng. J. 99, 59–68.

Oliveira, M.S.N., Fitch, A.W., Ni, X., 2003. A study of bubble velocity and bubble residence time in a gassed oscillatory baffled column: effect of oscillation frequency. Chem. Eng. Res. Des. 81 (2), 233–242.

Oliveira, M.S.N., Fitch, A.W., Ni, X.-W., 2003. A study of velocity and residence time of single bubbles in a gassed oscillatory baffled column: effect of oscillation amplitude. J. Chem. Technol. Biotechnol. 78 (2–3), 220–226.

Quicker, G., Schumpe, A., Deckwer, W.-D.D., 1984. Gas-liquid interfacial areas in a bubble column with suspended solids. Chem. Eng. Sci. 39, 179–183.

Reis, N.M.F., 2006. Novel Oscillatory Flow Reactors for Biotechnological Applications (Ph.D. thesis). Minho University.

Reis, N., Mena, P., Vicente, A., Teixeira, J., Rocha, F., 2007. The intensification of gas-liquid flows with a periodic, constricted oscillatory-meso tube. Chem. Eng. Sci. 62 (24), 7454–7462.

Sada, E., Kumazawa, H., Lee, C., Fujiwara, N., 1985. Gas-liquid mass transfer characteristics in a bubble column with suspended sparingly soluble fine particles. Ind. Eng. Chem. Process Des. Dev. 24 (2), 255–261.

Sada, E., Kumazawa, H., Lee, C., Iguchi, T., 1986. Gas holdup and mass transfer characteristics in a three-phase bubble column. Ind. Eng. Chem. Process Des. Dev. 25 (2), 472–476.

Smith, K.B., 1999. The Scale-Up of Oscillatory Flow Mixing (Ph.D. thesis). University of Cambridge.

Vasconcelos, J., Alves, S.S., Barata, J.M., 1995. Mixing in gas-liquid contactors agitated by multiple turbines. Chem. Eng. Sci. 50 (14), 2341–2354.

Warsito, Ohkawa, M., Maezawa, A., Uchida, S., Ohkawa, M., 1997. Flow structure and phase distributions in a slurry bubble column. Chem. Eng. Sci. 52 (21–22), 3941–3947.

Yoo, D.H., Tsuge, H., Terasaka, K., Mizutani, K., 1997. Behavior of bubble formation in suspended solution for an elevated pressure system. Chem. Eng. Sci. 52, 3701–3707.

Zhang, J.P., Grace, J.R., Epstein, N., Lim, K.S., 1997. Flow regime identification in gas-liquid flow and three-phase fluidized beds. Chem. Eng. Sci. 52, 3979–3992.